C Journal of Carbon Research

MDPI

Article

Effect of Halogen Ions on the Photocycle of Fluorescent Carbon Nanodots

Alice Sciortino [1], Roberto Pecorella [1], Marco Cannas [1] and Fabrizio Messina [1,2,*]

[1] Dipartimento di Fisica e Chimica—Emilio Segrè, Università degli studi di Palermo, via Archirafi 36, 90100 Palermo, Italy; alicesciortino@gmail.com (A.S.); pecorella.roberto@gmail.com (R.P.); marco.cannas@unipa.it (M.C.)

[2] CHAB-ATeN Center, Università degli studi di Palermo, Viale delle Scienze, Edificio 18, 90128 Palermo, Italy

* Correspondence: fabrizio.messina@unipa.it; Tel.: +39-09123891773

Received: 29 September 2019; Accepted: 22 October 2019; Published: 24 October 2019

Abstract: Carbon dots (C-dots) are well-known for their strong sensitivity to the environment, which reflects on intensity and shape changes of their fluorescence, induced by various interacting ions and molecules in solution. Although these interactions have been extensively studied in the last few years, especially in view of their possible sensing applications, the existing works have mostly focused on the quenching of C-dot fluorescence induced by metal cations. In fact, these latter easily bind to C-dots surfaces, which are negatively charged in most cases, promoting an electron transfer from the surface to them. Much less is known from the literature on the effect induced on C-dots by prototypical negative species in solutions, motivating more systematic studies on this different class of interactions. Here, we analyzed the effect of halogen ions on the fluorescence of C-dots, by combining steady-state optical absorption and photoluminescence, time-resolved fluorescence and femtosecond pump/probe spectroscopy. We demonstrate a quenching effect of C-dots fluorescence in the presence of halogen ions, which becomes more and more pronounced with increasing atomic number of the halogens, being negligible for chloride, appreciable for bromide and stronger for iodide. We find that quenching is mostly static, due to the binding of halogen ions on suitable surface sites at C-dots surfaces, while collisional quenching becomes obvious only at very high iodide concentrations. Finally, nanosecond and femtosecond time-resolved spectroscopies provide information on the quenching mechanism and time scales. Based on these data, we propose that the fluorescent state is deactivated by intersystem crossing to a dark triplet state, induced by close-range interactions with the heaviest halogen ions.

Keywords: carbon nanodots; fluorescence quenching; heavy atom effect; ultrafast transient absorption; quenching

1. Introduction

In recent years, fluorescent carbon nanoparticles (carbon nanodots—C-dots) have become a very debated topic in nanomaterial science due to their interesting optical characteristics [1–4]. Beyond their non-toxicity, ease of synthesis, highly functionalized surface, very versatile structural properties [5–8] and significant two photon absorption properties [9], C-dots usually display an intense fluorescence due to the radiative recombination of an electron with hole after photo-excitation, usually occurring on surface trap sites [1,10–12] although not always [13]. This fluorescence is very sensitive to the external environment and strongly responds to changes in environmental parameters, as for example solvent polarity [10,14], or the presence of molecules or ions in solution [12,15–17], leading to the use of C-dots as sensors in solution phase. Therefore, plenty of optical investigations of the interaction between C-dots and ions or molecules in solution exist in the literature. In particular, it is very common to propose C-dots as nanosensors of metal cations in solution [15,17,18] because photoexcited

C-dots display a negatively charged surface, to which metal cations as Cu^{2+}, Co^{2+} and Fe^{3+} easily bind, leading to measurable changes in C-dots optical spectra. Therefore, these interactions have been thoroughly studied leading to a deep understanding of the underlying photophysics, typically involving picosecond and sub-picosecond electron transfer [15,19]. On the contrary, much less is known about the interaction between C-dots and negative ions in solution, which is probably controlled by very different basic phenomena. Moreover, it is worth noting that the few studies of the interactions between C-dots and anions [20–24] were carried out through an indirect approach. In fact, the authors have been forced to use the interaction between C-dots and cations in order to reveal the interaction of C-dots with negative ions. For instance, reference [21] proposed a sensing scheme of S^{2-} anions based on their ability to bind Cu^{2+} ions and restore the emission of CDs, initially quenched by Cu^{2+}.

Here, we report a study of the influence of halogen ions on the fluorescence of C-dots, conducted by the combined use of steady-state and time-resolved optical methods. We show that halogen induce on C-dots a fluorescence quenching effect, the efficiency of which systematically increases with the atomic number of the halogen, being negligible for chloride, significant for bromide and more significant for iodide. This behavior points to a quenching driven by heavy-atom-induced intersystem crossing to dark triplet states. By time-resolved spectroscopic techniques, we found out that the quenching of the emission is static and due to the formation of C-dots-halogen complexes. The static-type interactions prevail until a certain amount of ions is added in solution, suggesting that saturation is reached in the available binding sites on the surface of C-dots. Overcoming this threshold value gives the start to a collisional quenching regime, leading to a further decrease of the fluorescence intensity. Moreover, by femtosecond ultrafast technique it was possible to investigate the typical dynamics of photoexcited C-dots comparing it to C-dots-ions complexes. The results are consistent with a heavy-atom effect interpretation of the observed quenching, and suggest that it occurs on a time scale of a few hundred picoseconds.

2. Materials and Methods

Carbon nanodots were synthesized by an induced microwave thermal decomposition of an aqueous solution of citric acid and urea (in a 1:1 weight ratio) as previously reported [25].

Infrared absorption spectra have been recorded on a N_2-purged VERTEX-70 spectrophotometer (Bruker, Billerica, MA, USA) in transmission geometry. Samples have been prepared by drop casting a C-dots solution on a sapphire window. All the measurements have been performed at room temperature under a continuous flux of nitrogen, which avoid residual water artifacts.

Atomic force microscopy (AFM) measurements were performed in air by using a FAST-SCAN microscope (Bruker, Billerica, MA, USA) equipped with a closed-loop scanner (X, Y and Z maximum scan ranges 35 μm, 35 μm and 3 μm respectively). The scans were obtained in soft tapping mode by using FAST-SCAN-A probes with an apical radius of about 5 nm. Every image has been recorded with a pixel resolution comparable to the tip size. The samples have been prepared by the drop casting on a mica substrate a drop of C-dots solution.

Optical absorption spectra were recorded on solutions of C-dots in water in 1 cm quartz cuvettes, by using an optical fiber spectrophotometer (AVANTES, Apeldoorn, The Netherlands) equipped with a double halogen/deuterium lamp and a CCD detector. The measurements were performed at room temperature.

The emission spectra were recorded on aqueous solutions by a FP-6500 spectrofluorometer (JASCO, Tokyo, Japan) in 1 cm quartz cuvettes with a 3 nm resolution bandwidth. All the measurements have been performed with the same experimental parameters in order to compare directly the emission bands. The measurements were performed at room temperature.

Time-resolved fluorescence spectra were recorded by an intensified CCD camera (Princeton, NJ, USA) capable of acquiring the emission spectrum within temporal windows of 0.5 ns, variably delayed after the laser pulse. The emission was excited by 5 ns pulses of <1.0 mJ energy provided by a tunable laser system consisting in an OPO (optical parametric oscillator), which is pumped by

the third harmonic of a pulsed Q-switched Nd:YAG laser. The laser provided pulses in the visible (410–700 nm) range. The time resolution was about 2–3 ns.

Femtosecond transient absorption (TA) measurements were based on a 5 kHz Ti:sapphire femtosecond amplifier (Spectra Physics, Santa Clara, CA, US), which produces 75 fs pulses peaking at 800 nm, having a full width at half maximum (FWHM) of 30 nm, and 350 μJ energy/pulse. This beam was split in two parts by a beam splitter (80%/20%) to generate the pump and the probe, respectively. The pump (400 nm) was produced from the fundamental 800 nm by frequency doubling in an ultrathin β−BBO crystal (250 μm). The 400-beam was chopped at 500 Hz and focused on the sample by a parabolic mirror with f = 150 mm. Its polarization was controlled by a waveplate. On the second arm, a supercontinuum pulse (the probe, 400–700 nm) was generated by focusing the 800 nm beam in a 1 mm quartz cuvette containing D_2O. The probe was focused on the sample by the same parabolic mirror used to focus the pump. The pump–probe delay was controlled by a motorized delay stage, which guarantees a temporal resolution of 70 fs. The probe and the pump overlap within the sample, which continuously flows in a 200 μm thick flow cell upon the action of a peristaltic pump in order to be sure that every pump pulse hits a fresh portion of the sample.

After the sample, the probe beam was dispersed through a Brewster-angle silica prism and focused on the detector by a lens. The spectral resolution was 3 nm. Pump and probe were synchronized with a camera detector system with 1024 pixels with single-shot capability. A typical signal was obtained by averaging 5000 pumped and 5000 unpumped spectra for each delay, and scanning over the pump–probe delay 20 times.

3. Results and Discussion

Morphological characterization of C-dots was performed by AFM measurements. The size distribution, obtained by sampling about 1000 dots, is reported in Figure 1a. These data show that these C-dots were nanoparticles with average diameter of about 4 nm. By infrared absorption measurements (Figure 1b) we found out that, as expected, the surface of these carbon nanoparticles was full of various polar groups as carboxylic groups (peak at 1700 cm^{-1}) and amide groups (1670–1600 cm^{-1}).

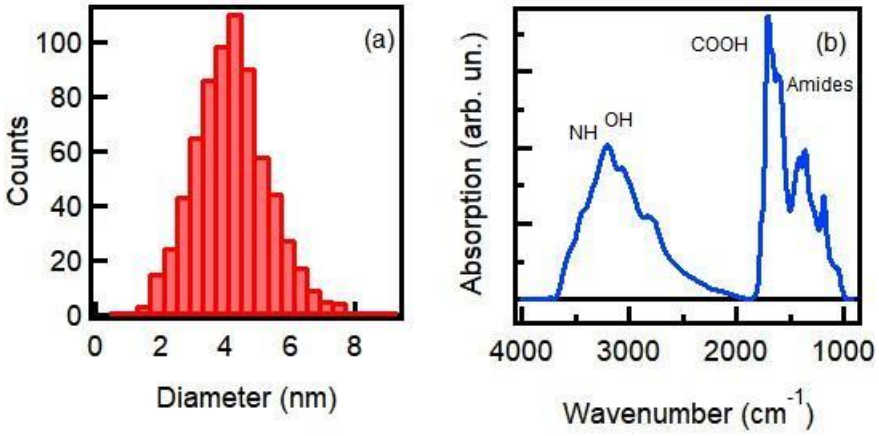

Figure 1. (**a**) Size distribution of C-dots from atomic force microscopy (AFM) measurements. (**b**) Infrared absorption spectrum of C-dots. The labels point out the attributions that we propose for the absorption peaks. The vibrational signals are associated to amide (1670–1600 cm^{-1}), carboxylic groups (1700 cm^{-1}) and hydroxyl groups (3200 cm^{-1}), which cover C-dots surfaces.

The absorption spectrum of an aqueous solution of C-dots is reported in Figure 2. It displays two absorption peaks at 340 nm and at 400 nm, combined with an absorption tail at longer wavelengths. The latter is very typical for N-doped C-dots and represents a family of emissive electronic transitions, which is responsible for the typical tunability of C-dots emission, that is, their characteristically excitation-dependent fluorescence [26].

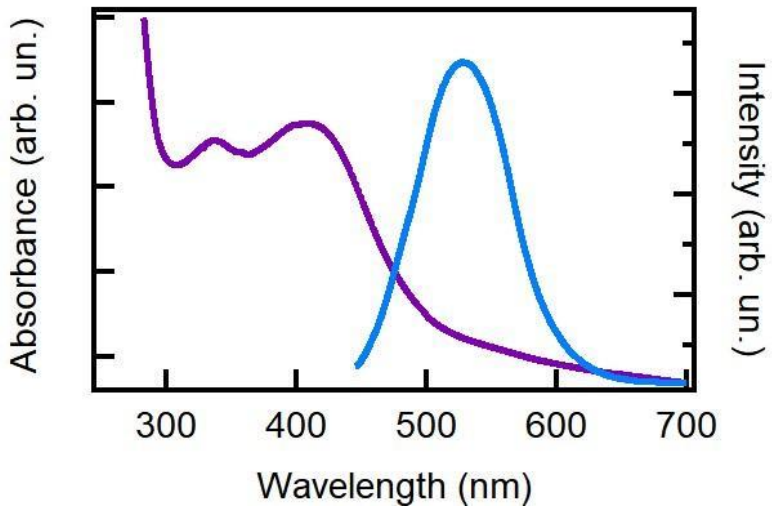

Figure 2. Absorption spectrum of an aqueous solution of C-dots (purple curve) and steady-state emission spectrum of C-dots excited at 440 nm (blue curve).

In particular, exciting the C-dots solution at 440 nm produces an emission band peaking at 530 nm, as shown in Figure 2, which displays a quantum yield (QY) of 13% [10] as we estimate by comparing the steady-state emission intensity with a reference sample (fluorescein in water, pH = 11 and QY = 95%). We dissolved in C-dots solution different amounts of various salts of the following halogen ions: Cl^-, Br^- and I^-, in order to investigate the resulting changes in C-dots optical properties.

As shown in Figure 3a, C-dots in a 10 mM aqueous solution of KCl or KBr display the same intensity and the same emission shape with respect to bare C-dots. This clearly indicates that at this concentration neither Cl^- nor Br^- were able to inhibit the fluorescence. On the contrary, if C-dots interact with KI, their emission was affected by an intensity decrease of 20% (red spectrum in Figure 3a). This highlights that: i) among the three halogens, at this concentration only iodide ions significantly interacted with C-dots and ii) the emission was not affected by the presence of the potassium ions. In order to fully assess the effect of the counterions we also recorded the emission spectra of C-dots in the presence of 10 mM of NaCl and NaI salts. As shown in Figure 3a, NaCl did not modify the emission band, which was the same result we found for KCl, and NaI produced the exact same effect with respect to the KI, that was a 20% quenching. Overall, these results demonstrated the negligible influence of alkali metal ions on the emission of C-dots, and confirm the effect of I^- as a quencher among the three halogen ions.

Increasing the amount of salt in solution up to 100 mM provides more information on the effect of the various halogen ion, and how they compare to each other. In fact, as shown in Figure 3b, 100 mM Cl^- still did not influence the emission at all (blue spectrum), 100 mM of Br^- quenched the intensity of about 20% and 100 mM of I^- caused a 65% of quenching. Considering the regular progression of the atomic number in the isoelectronic series of the three ions, these results suggest that the quenching mechanism was driven by a so-called heavy atom effect, a common quenching mechanism for many molecular dyes [27,28]. In other words, this quenching suggests a transition of C-dots to a dark triplet state, due to intersystem crossing (ISC) induced by the close-range interaction with an atom with a high atomic number. Anyway, no new phosphorescence signal grows up in the steady-state measurements, indicating that the quantum yield of the triplet state was practically close to zero, because of the very low radiative rate.

As an alternative to an ISC process, quenching could theoretically be due to an electron transfer from the halogen anion to the C-dots. However, this mechanism seems very unlikely considering the nature of the optical transition of these C-dots: as previously reported [10], photoexcitation of these C-dots leads to a charge separation event forming an electron trapped on a surface site (exposed to the environment), while the positive hole stays well-buried inside the core, not exposed to the solvent.

Therefore, it seems unlikely that the C-dots are readily available to accept an electron from the anion, supposedly recombining with the positive hole in the core [10].

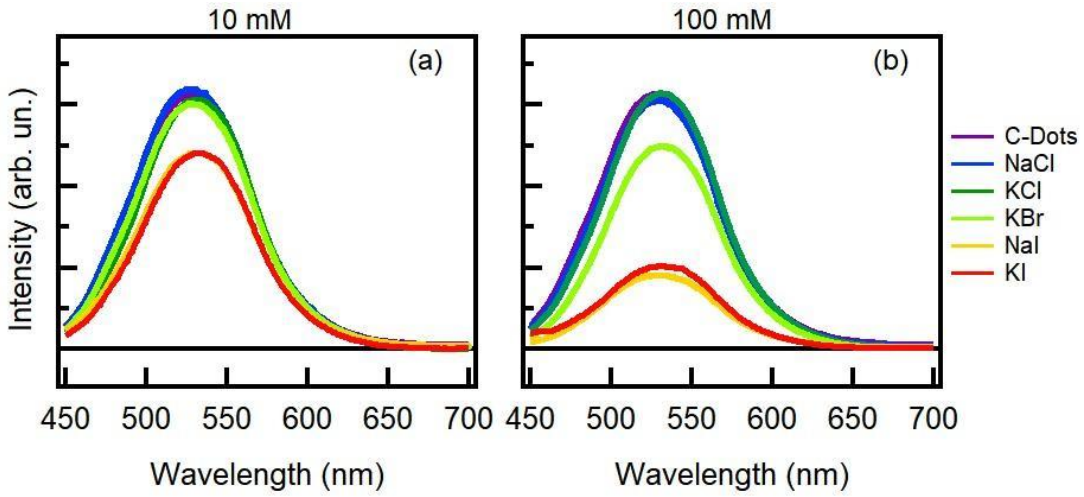

Figure 3. Emission spectra of bare C-dots (purple curve, both panels), of C-dots with 10 mM of salt (**a**) and with 100 mM of salt (**b**). Salt list: NaCl (blue curves), KCl (dark green curves), KBr (light green curves), NaI (Yellow curve) and KI (red curves).

To deeply understand the quenching mechanism, it is mandatory to analyze its dynamics over different time scales. For this reason, we investigated the emission by time resolved methods, first with nanosecond resolution, then with femtosecond resolution. In Figure 4, the decay kinetics of C-dots emission bands are reported, along with their best fitting curves. The function used to fit the kinetics is a stretched exponential $f(t) = A{\cdot}e^{-((t/\tau)^b)}$ where is the fluorescence lifetime and b is the stretching parameter, which quantifies the degree of inhomogeneity of the emissive ensemble, due to the large dot-to-dot fluctuations observed for C-dots [26,29]. Excluding the case of C-dots in the presence of 100 mM iodide, the data in Figure 4 show that all the measured kinetics are identical within experimental uncertainty. In fact, the fitting procedure gives the same lifetime ($\tau_0 = 5 \pm 0.3$ ns) and the same stretching parameter (0.90 ± 0.05) for all the samples. In particular, there are no significant differences between the decay kinetics of bare C-dots and the kinetics of C-dots with 100 mM Br^- ions, despite an obvious steady-state emission quenching (Figure 3b). This indicates that in this case the quenching is purely static, that is, occurring within a stable C-Dot-Br^- complex pre-existing to photo-excitation. The same situation happens for 10 mM of I^-: same lifetime with respect to bare C-dots but a steady state quenching of 20%.

Due to the abundance of surface carboxylic acid moieties, most C-dots in aqueous solution are characterized by negative surface charge [3], so that the formation of stable complexes with negative halogen ions may appear surprising. However, the surface structure of C-dots is highly complex and very disordered, and our previous infrared and XPS studies of these dots revealed the presence of at least one type of positively charged surface group, specifically an amide with a protonated nitrogen [25]. Therefore, it is likely that the halogen anions get electrostatically attached to these positive portions of the dots surface, where they inhibit the fluorescent radiative recombination of photo-excited electron-hole pairs.

The situation was different when C-dots interacted with 100 mM of I^- ions. In fact, when the amount of these ions increased of an order of magnitude the emission lifetime of C-dots decreased to 2.4 ns (see Figure 4), which is the fingerprint of a collisional quenching mechanism. The measured decrease in lifetime corresponds to a ratio $\tau_0/\tau = 2.2$, which was very close to the ratio $I_0/I_{100\ mM\ I} = 2.7$ between steady-state intensities in Figure 3b. This match indicates that at 100 mM concentration, the quenching induced by iodide ions is mostly dynamic [27]. However, considering the previous

conclusion that 10 mM iodide anions induced a purely static quenching (Figures 3a and 4), we could certainly say that at [I^-] = 100 mM the quenching could not be "purely" collisional. In fact, the ratio between lifetimes was exactly identical to the ratio $I_{10\ mM\ I}/I_{100\ mM\ I}$ = 2.2 between the intensities in the presence of 10 mM and 100 mM iodide concentrations. This suggests that beyond a first static quenching regime controlled by the formation of non-luminescent C-dots-I^- complexes, there is a second quenching regime due to pure collisions, which is only observed at higher concentration. As already mentioned above, and frequently reported [2,4], only a minority of CD surface groups display a positive charge. Therefore, it is not surprising that a relatively small concentration of 10 mM iodide ions was enough to saturate all the available sites to bind the ions to C-dots surfaces and form non-emissive complexes. Once these sites are saturated, further quenching can only occur dynamically through collisions.

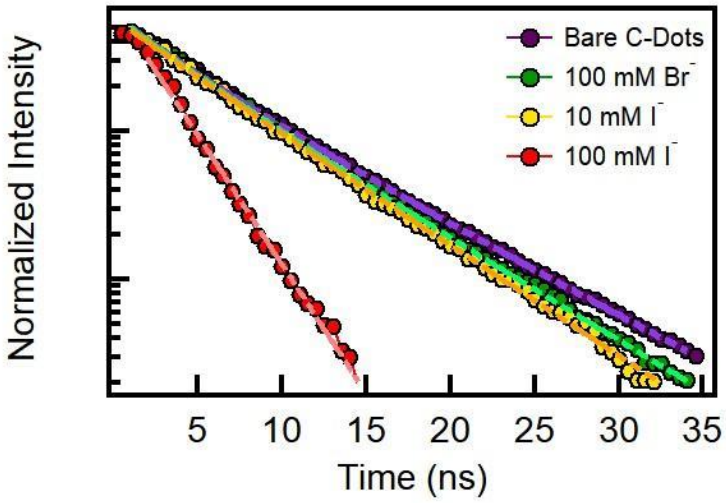

Figure 4. Normalized decay fluorescence excited at 440 nm of bare C-dots (purple curve), of C-dots with 100 mM of Br^- (green curve), with 10 mM (yellow curve) and 100 mM (red curve) of I^- with the respective least-squares fitting curves.

Since static quenching regime is characterized by lack of changes of the nanosecond decay kinetics (Figure 4), the photophysical interaction responsible for quenching mostly occurs on a faster time range, similar to what observed in other cases. For example, in complexes of C-dots with metal cations, quenching is driven by electron transfer from C-dots to the cation, and the resulting timescales are very fast (0.2–2 ps) [15]. Here, where quenching is driven by the heavy-atom effect, it is very difficult to make a defined prediction on the time scale on which the quenching photochemical event should occur. In fact, depending on the system, the characteristic time scale of ISC can vary over several orders of magnitude ranging from <100 fs for metal complexes [28,30] to several nanoseconds. Therefore, we performed femtosecond transient absorption measurements to further study the photophysics of these complexes and to discriminate the possible phenomena that could theoretically explain the quenching, as an ISC or a charge transfer between C-dots and halogen ions. Femtosecond measurements, shown in Figure 5, were carried out on solutions of C-dots with and without 10 mM iodide ions.

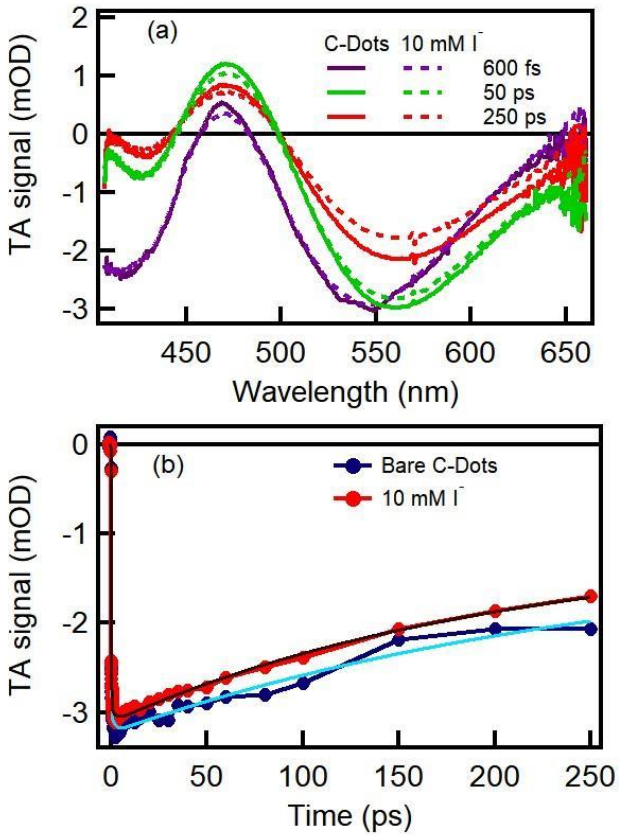

Figure 5. (**a**) Normalized transient absorption spectra of a solution of bare C-dots (continuous lines) and of a solution of C-dots with 10 mM iodide ions (dashed lines), recorded at 600 fs (purple lines), 50 ps (green lines) and 250 ps (red lines) delays after photo-excitation at 400 nm. (**b**) Kinetic traces at 550 nm (peak of stimulated emission), extracted from the data in panel a for bare C-dots (blue lines) and C-dots with 10 mM of iodide (red line), respectively, and their best fitting curves.

After photoexcitation at 400 nm, a solution of bare C-dots shows a transient signal with similar shape at every delays (Figure 5a): (i) a negative signal around 400 nm (pump wavelength) due to a ground state bleaching (GSB), (ii) a positive signal around 470 nm related to electronic transitions from the excited state (ESA) and (iii) a broad negative signal, which peaks at 550 nm due to the stimulated emission (SE), which resembles the steady state emission in Figure 2 (although reversed in sign), as already observed in our previous work [15]. The dynamics observed for bare C-dots mostly consist of a partial decay of the GSB signal, together with a red shift and partial decay of the SE. Since our main goal here is to identify the effects induced by I^- ions, details of this dynamics will not be further discussed. The most important point here was that a direct comparison of bare C-dots TA data and those of C-dots interacting with 10 mM of iodide shows that they were essentially identical, both in regard to the shape of the spectra (Figure 5a) and to the kinetics of the SE signal, shown in Figure 5b. These results strongly suggest that the quenching event and the consequent population of a dark state occurred after the end of the temporal range explored by the TA measurements, that is, they are slower than ~250 ps. In particular, the almost identical shape of the TA signal in the two samples, and the absence of any new ESA signal potentially arising from the photoproduct of the quenching reaction, indicate that the ISC to a dark triplet state has not yet occurred within the first ~250 ps after photo-excitation. Unfortunately, the femtosecond pump/probe measurements did not allow us to fully cover the time range of several hundreds of picoseconds, which would be needed to thoroughly sample this process, which is also too fast to be investigated by nanosecond-resolved measurements. Although we could not conclusively identify the time scale of ISC, our results narrow it down in the

range between ~250 ps (the limit of the TA scan) and ~2 ns, that is the temporal resolution of the nanosecond setup.

We also carried out a least-square fitting of the kinetic traces with a multi-exponential function convoluted to our instrumental response function, as explained elsewhere [15]. We found that the dynamics were satisfactorily described by three time scales τ_1, τ_2 and τ_3: the faster time constants in bare and in iodide C-dots were the same (τ_1 ~0.2 ps and τ_2 ~2 ps), and so were the amplitudes $A_1 = (1.4 \pm 0.2) \times 10^{-3}$ and $A_2 = (0.20 \pm 0.05) \times 10^{-3}$. As for the slowest process, the amplitude $A_3 = -(2.0 \pm 0.2) \times 10^{-3}$ is the same, while the time scale was slightly different in the two samples, being $\tau_3 = 250 \pm 30$ ps for bare C-dots and $\tau_3 = 200 \pm 30$ ps for C-dots with halogen atoms.

The coincidence of the amplitudes obtained from the fit indicates that the excited portion of the sample at time zero was the same for both experiments, suggesting once again that the transition to a dark state occurs at long delays after the photoexcitation, rather than within our temporal resolution of 100 fs. Besides, the difference between the time scales of the long component (200 ps vs. 250 ps), which becomes faster in the presence of iodide, may suggest the earliest onset of iodide-induced ISC, although further experiments extending to several hundred ps would be needed to confirm this conclusion.

4. Conclusions

The interactions between C-dots and halogen atoms were investigated by various spectroscopic techniques with different time resolution. The close contact between C-dots and halogen anions produces a quenching of the emission, which increased with the increase of the atomic number of the anion, suggesting a heavy-atom effect producing an intersystem crossing from the luminescent electronic state of the dot to its dark triplet state. This quenching was only significant at relatively high concentrations of halogen anions, much higher than typically observed in the literature for the quenching of C-dots by metal cations. This was likely due to the low abundance of suitable binding sites for the anions on C-dots surfaces. We also demonstrated that the quenching was purely static until the negative ions were completely attached to the few positive groups on the dot surface, saturating them. Beside this threshold, further quenching proceeds via a collisional mechanism. Finally, we carried out femtosecond investigations comparing the ultrafast photocycle of C-dots with and without the addition of iodide ions. Despite these measurements did not allow us to identify the precise time scale on which ISC occurs, they allowed us to narrow it down to a specific temporal range, between ~250 ps and ~2 ns.

Author Contributions: F.M. and A.S. conceived and designed the study, and built the femtosecond pump-probe setup. A.S. and R.P. performed the experiments and analyzed the data. F.M. supervised and validated the experiments. A.S. and F.M. wrote the paper draft. A.S., R.P., M.C. and F.M. discussed the interpretation of the data and revised the paper to its final form.

Funding: This research received no external funding.

Acknowledgments: We thank the Laboratory "Roberto Boscaino" of Advanced Materials (LaBAM) group (www.unipa.it/lamp) at University of Palermo for support and stimulating discussions.

Conflicts of Interest: The authors declare no conflict of interest

References

1. Sun, Y.; Zhou, B.; Lin, Y.; Wang, W.; Fernando, K.A.S.; Pathak, P.; Meziani, M.J.; Harruff, B.A.; Wang, X.; Wang, H.; et al. Quantum-sized carbon dots for bright and colorful photoluminescence. *J. Am. Chem. Soc.* **2006**, *128*, 7756–7757. [CrossRef] [PubMed]
2. Li, H.; Kang, Z.; Liu, Y.; Lee, S.T. Carbon nanodots: Synthesis, properties and applications. *J. Mater. Chem.* **2012**, *22*, 24230–24253. [CrossRef]
3. Sciortino, A.; Cannizzo, A.; Messina, F. Carbon nanodots: A review—From current understanding of the fundamental photophysics to the full control of the optical response. *C* **2018**, *4*, 67. [CrossRef]
4. Hola, K.; Zhang, Y.; Wang, Y.; Giannellis, E.P.; Zboril, R.; Rogach, A.L. Carbon dots-Emerging light emitters for bioimaging, cancer therapy and optoelectronics. *Nanotoday* **2014**, *9*, 590–603. [CrossRef]

5. Sahu, S.; Behera, B.; Maiti, T.K.; Mohapatra, S. Simple one-step synthesis of highly luminescent carbon dots from orange juice: Application as excellent bio-imaging agents. *Chem. Commun.* **2012**, *48*, 8835–8837. [CrossRef] [PubMed]
6. Liu, S.; Tian, J.; Wang, L.; Zhang, Y.; Qin, X.; Luo, Y.; Asiri, A.M.; Al-Youbi, A.O.; Sun, X. Hydrothermal treatment of grass: A low-cost, green route to nitrogen-doped, carbon-rich, photoluminescent polymer nanodots as an effective fluorescent sensing platform for label-free detection of Cu(II) ions. *Adv. Mater.* **2012**, *24*, 2037–2041. [CrossRef]
7. Cayuela, A.; Soriano, M.L.; Carrillo-Carrion, C.; Valcarcel, M. Semiconductor and carbon-based fluorescent nanodots: The need for consistency. *Chem. Commun.* **2016**, *52*, 1311–1326. [CrossRef] [PubMed]
8. Chandra, S.; Pathan, S.H.; Mitra, S.; Modha, B.H.; Goswami, A.; Pramanik, P. Tuning of photoluminescence on different surface functionalized carbon quantum dots. *RSC Adv.* **2012**, *2*, 3602–3606. [CrossRef]
9. Santos, C.I.M.; Mariz, I.F.A.; Pinto, S.N.; Gonçalves, G.; Bdikin, I.; Marques, P.A.A.P.; Neves, M.G.P.M.S.; Martinho, J.M.G.; Maçoas, E.M.S. Selective two-photon absorption in carbon dots: A piece of the photoluminescence emission puzzle. *Nanoscale* **2018**, *26*, 12505–12514. [CrossRef]
10. Sciortino, A.; Marino, E.; van Dam, B.; Schall, P.; Cannas, M.; Messina, F. Solvatochromism unravels the emission mechanism of carbon nanodots. *J. Phys. Chem. Lett.* **2016**, *7*, 3419–3423. [CrossRef]
11. Zhu, S.; Wang, L.; Bo, L.; Song, Y.; Zhao, X.; Zhang, G.; Zhang, S.; Lu, S.; Zhang, J.; Wang, H.; et al. Investigation of photoluminescence mechanism of graphene quantum dots and evaluation of their assembly into polymer dots. *Carbon* **2014**, *77*, 462–472. [CrossRef]
12. Wang, X.; Cao, L.; Lu, F.; Meziani, M.J.; Li, H.; Qi, G.; Zhou, B.; Harruff, B.A.; Kermarrec, F.; Sun, Y.-P. Photoinduced electron transfers with carbon dots. *Chem. Commun.* **2009**, 3774–3776. [CrossRef] [PubMed]
13. Malyukin, Y.; Viagin, O.; Maksimchuk, P.; Dekaliuk, M.; Demchenko, A. Insight into the mechanism of the photoluminescence of carbon nanoparticles derived from cryogenic studies. *Nanoscale* **2018**, *10*, 9320–9328. [CrossRef] [PubMed]
14. Kundu, A.; Park, B.; Oh, J.; Sankar, K.V.; Ray, C.; Kim, W.S.; Jun, S.C. Multicolor emissive carbon dot with solvatochromic behaviour across the entire visible spectrum. *Carbon* **2020**, *156*, 110–118. [CrossRef]
15. Sciortino, A.; Madonia, A.; Gazzetto, M.; Sciortino, L.; Rohwer, E.J.; Feurer, T.; Gelardi, F.M.; Cannas, M.; Cannizzo, A.; Messina, F. The interaction of photoexcited carbon nanodots with metal ions disclosed down to the femtosecond scale. *Nanoscale* **2017**, *9*, 11902–11911. [CrossRef]
16. Fresco-Cala, B.; Soriano, M.L.; Sciortino, A.; Cannas, F.; Messina, F.; Cardenas, S. One-pot synthesis of graphene quantum dots and simultaneous nanostructured self-assembly via a novel microwave-assisted method: Impact on triazine removal and efficiency monitoring. *RSC Adv.* **2018**, *8*, 29939–29946. [CrossRef]
17. Xu, X.; Ren, D.; Chai, Y.; Cheng, X.; Mei, J.; Bao, J.; Wei, F.; Xu, G.; Hu, Q.; Cen, Y. Dual-emission carbon dots-based fluorescent probe for ratiometric sensing of Fe(III) and pyrophosphate in biological samples. *Sens. Actuators B Chem.* **2019**, *298*, 126829. [CrossRef]
18. Desai, M.L.; Basu, H.; Saha, S.; Singhal, R.K.; Kailasa, S.K. Investigation of silicon doping into carbon dots for improved fluorescence properties for selective detection of Fe^{3+} ion. *Opt. Mater.* **2019**, *96*, 109374. [CrossRef]
19. Strauss, V.; Margraf, J.T.; Dolle, C.; Butz, B.; Nacken, T.J.; Walter, J.; Bauer, W.; Peukert, W.; Spiecker, E.; Clark, T.; et al. Carbon nanodots: Toward a comprehensive understanding of their photoluminescence. *J. Am. Chem. Soc.* **2014**, *136*, 17308–17316. [CrossRef]
20. Zhao, H.X.; Liu, L.Q.; Liu, Z.D.; Wang, Y.; Zhao, X.J.; Huang, C.Z. Highly selective detection of phosphate in very complicated matrixes with an off-on fluorescent probe of europium-adjusted carbon dots. *Chem. Commun.* **2011**, *47*, 2604–2606. [CrossRef]
21. Hou, X.; Zeng, F.; Du, F.; Wu, S. Carbon-dot-based fluorescent turn-on sensor for selectively detecting sulphide anions in totally aqueous media and imaging inside live cells. *Nanotechnology* **2013**, *24*, 335502. [CrossRef] [PubMed]
22. Hu, Y.; Yang, J.; Jia, L.; Yu, J.S. Ethanol in aqueous hydrogen peroxide solution: Hydrothermal synthesis of highly photoluminescent carbon dots as multifunctional nanosensors. *Carbon* **2015**, *93*, 999–1007. [CrossRef]
23. Zhao, D.; Chen, C.; Lu, L.; Yang, F.; Yang, X. A dual-mode colorimetric and fluorometric "light on" sensor for thiocyanate based on fluorescent carbon dots and unmodified gold nanoparticles. *Analyst* **2015**, *140*, 8157–8164. [CrossRef]
24. Dhenadhayalan, N.; Lin, K.-C. Chemically induced fluorescence switching of carbon-dots and its multiple logic gate implementation. *Sci. Rep.* **2015**, *5*, 10012. [CrossRef] [PubMed]

25. Messina, F.; Sciortino, L.; Popescu, R.; Venezia, A.M.; Sciortino, A.; Buscarino, G.; Agnello, S.; Schneider, R.; Gerthsen, D.; Cannas, M.; et al. Fluorescent nitrogen-rich carbon nanodots with an unexpected b-C3N4 nanocrystalline structure. *J. Mater. Chem. C* **2016**, *4*, 2598–2605.
26. Sciortino, A.; Gazzetto, M.; Buscarino, G.; Popescu, R.; Schneider, R.; Giammona, G.; Gerthsen, D.; Rohwer, E.J.; Mauro, N.; Feurer, T.; et al. Disentangling size effects and spectral inhomogeneity in carbon nanodots by ultrafast dynamical hole-burning. *Nanoscale* **2018**, *10*, 15317–15323. [CrossRef]
27. Lakowicz, R. *Principles of Fluorescence Spectroscopy*; Springer Science: Berlin, Germany, 2006.
28. Penfold, T.J.; Gindersperger, E.; Daniel, C.; Marian, C.M. Spin-Vibronic mechanism for intersystem crossing. *Chem. Rev.* **2018**, *118*, 6975–7025. [CrossRef]
29. Demchenko, A.P.; Dekaliuk, M.O. The origin of emissive states of carbon nanoparticles derived from ensemble-averaged and single-molecular studies. *Nanoscale* **2016**, *8*, 14057–14069. [CrossRef]
30. Messina, F.; Pomarico, E.; Silatanai, M.; Baranoff, E.; Chergui, M. Ligand-centered fluorescence and electronic relaxation cascade at vibrational time scales in transitions-metal complexes. *J. Phys. Chem. Lett.* **2015**, *6*, 4475–4480. [CrossRef]